

# Probing an effective-range-induced super fermionic Tonks-Girardeau gas with ultracold atoms in one-dimensional harmonic traps

Xiao-Long Chen, Xia-Ji Liu, and Hui Hu\*

Centre for Quantum and Optical Science, Swinburne University of Technology, Melbourne, Victoria 3122, Australia

(Dated: July 21, 2016)

We theoretically investigate an ultracold spin-polarized atomic Fermi gas with resonant odd-channel ( $p$ -wave) interactions trapped in one-dimensional harmonic traps. We solve the Yang-Yang thermodynamic equations based on the exact Bethe ansatz solution, and predict the finite-temperature density profile and breathing mode frequency, by using a local density approximation to take into account the harmonic trapping potential. The system features an exotic super fermionic Tonks-Girardeau (super-fTG) phase, due to the large effective range of the interatomic interactions. We explore the parameter space for such a fascinating super-fTG phase at finite temperature and provide smoking-gun signatures of its existence in both breathing mode frequencies and density profiles. Our results suggest that the super-fTG phase can be readily probed at temperature at about  $0.1T_F$ , where  $T_F$  is the Fermi temperature. These results are to be confronted with future cold-atom experiments with  $^6\text{Li}$  and  $^{40}\text{K}$  atoms.

PACS numbers: 03.65.Nk, 03.75.Kk, 05.30.-d, 67.85.-d

The beautiful exactly-solvable models in one dimensional (1D) systems provide us a better understanding of fascinating low-dimensional quantum many-body systems in nature [1]. Recently, remarkable experimental progresses in ultracold atoms make it possible to realize the quasi-1D geometry in laboratory [2–9], and therefore pave the way to test a number of exact theoretical predictions and to confirm the predicted intriguing many-body phenomena [10]. A well-known example is a 1D Bose gas with strongly repulsive interparticle interactions, where bosons can not penetrate each other and therefore their many-body wavefunction resembles that of free spinless fermions and vanishes whenever two bosons coincide at the same position [11]. This so-called Tonks-Girardeau (TG) gas has attracted enormous attention over the past few decades, both experimentally and theoretically [4, 5, 8, 10, 12–15]. To date, evidences of a TG gas have been clearly identified in a number of experimental observables, including the density profile, momentum distribution, and collective oscillations [4, 5, 8]. A highly-excited super-TG Bose gas, which was predicted to occur by rapidly switching the sign of the interaction strength [16, 17], has also been experimentally confirmed [8].

In this Letter, we consider the experimental observation of another fascinating many-body phenomenon, a super fermionic Tonks-Girardeau (super-fTG) gas. It was predicted to emerge in a spin-polarized Fermi gas with resonant odd-channel or  $p$ -wave interactions [18]. In sharp contrast to the TG or super-TG Bose gas, where the strongly correlated state is driven by a large scattering length, the super-fTG gas is caused by a non-negligible effective range of the interparticle interactions [18], which is rare in cold-atom experiments. To explore the realistic parameter space for observing the super-fTG gas at *finite* temperature, we exactly solve the Yang-

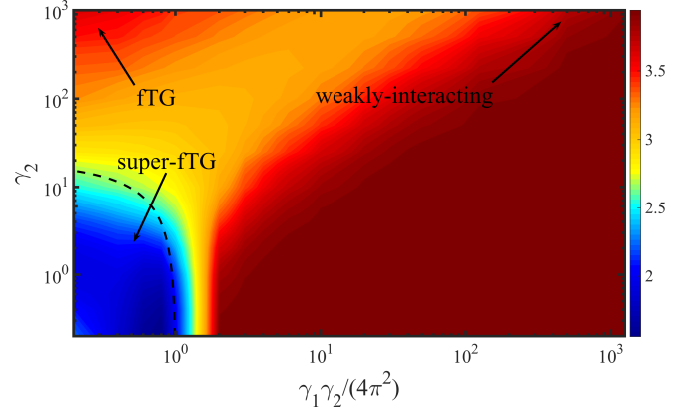


FIG. 1. (color online). Contour plot of the squared breathing mode frequency  $(\omega_b/\omega_{ho})^2$  as functions of the dimensionless interaction parameters  $\gamma_2$  and  $\gamma_1 \gamma_2 / (4\pi^2)$  (see the text for their definitions) in the logarithmic scale. The black dashed line is the zero-temperature analytic result Eq. (7) [18], indicating the transition into the super-fTG regime, either from the weakly interacting limit or the strongly interacting fTG limit. We have taken a typical temperature  $T = 0.1T_F$ .

Yang thermodynamic equations for the thermodynamics of the 1D  $p$ -wave Fermi gas based on the Bethe ansatz solution [19]. By taking into account the external harmonic potential with a trapping frequency  $\omega_{ho}$  via the local density approximation (LDA) [20], we calculate the finite-temperature density distribution of the Fermi cloud. By further using the two-fluid hydrodynamic theory [14, 21, 22], we determine the breathing mode frequency of the low-lying collective oscillations. Clear signatures of the appearance of a super-fTG gas in these two observables have been predicted.

Our main result is summarized in Fig. 1, where we report the dependence of the breathing mode frequency on the 1D scattering length (the horizontal axis) and ef-

fective range (the vertical axis) of the  $p$ -wave interaction, at a temperature  $0.1T_F$  that is typically available in cold-atom experiments. Three distinct regimes could be clearly identified: a weakly or strongly interacting Fermi gas with a mode frequency  $\omega_b \simeq 2\omega_{ho}$  and a super-fTG characterized by a much smaller mode frequency at large effective ranges (i.e.,  $\gamma_2 \rightarrow 0$ ). While the underlying quasiparticles in both weakly and strongly interacting regimes can be well interpreted in terms of fermions or bosons [10], the behavior of the compressible super-fTG state is more subtle to figure out. Therefore, the experimental observation of a super-fTG gas should provide a new opportunity to understand the challenging quantum many-body physics.

*1D  $p$ -wave atomic Fermi gases.* — We start by briefly reviewing the two-particle scattering property in a spin-polarized Fermi gas. Due to the Pauli exclusion principle, only odd-channel scatterings are possible, and at the low-energy limit, the  $p$ -wave scattering in three-dimensions (3D) is the strongest [23, 24]. Unlike the  $s$ -wave case, the  $p$ -wave scattering becomes energy-dependent, and an effective range of the interaction potential has to be included in order to regularize the contact interactions. The 3D  $p$ -wave scattering is then described by a phase shift  $\delta_p(k)$ :  $k^3 \cot \delta_p(k) = -1/w_1 - \alpha_1 k^2 + \mathcal{O}(k^4)$ , where  $k$  is the relative momentum of two colliding atoms, and  $w_1$  and  $\alpha_1$  are the scattering volume and effective range, respectively [23, 24]. For  ${}^6\text{Li}$  ( ${}^{40}\text{K}$ ) atoms, where the  $p$ -wave resonance occurs near  $B_0 = 215.0$  (198.8) G, the effective range  $\alpha_1$  is about 0.088 (0.021), in unit of inverse of Bohr radius ( $a_0^{-1}$ ) [25–28]. In the quasi-1D geometry considered here, where the transverse motion is completely suppressed by the strong transverse confinement potential using a two-dimensional optical lattice [3, 5, 6, 8], it is known that the 1D scattering amplitude in the odd channel (denoted as  $p$ -wave as well for convenience) takes the form [29, 30],

$$f_p^{\text{odd}}(k) = \frac{-ik}{1/l_p + \xi_p k^2 + ik}, \quad (1)$$

where  $l_p \approx 3a_\perp [a_\perp^3/w_1 - 3\sqrt{2}\zeta(-1/2)]^{-1}$  and  $\xi_p = \alpha_1 a_\perp^2/3 > 0$  are the 1D scattering length and effective range, respectively [18, 29, 30]. A confinement induced resonance appears when the 3D scattering length  $w_1^{1/3}$  is comparable to the transverse length  $a_\perp = \sqrt{\hbar/(m\omega_\perp)}$ , where  $m$  is the atomic mass and  $\omega_\perp$  is the trapping frequency of the transverse confinement [29–32].

*Yang-Yang thermodynamic equations.* — Ignoring the 1D effective range  $\xi_p$ , a 1D spin-polarized Fermi gas of  $N$  atoms is exactly solvable, owing to the fermion-boson duality [33, 34], which maps the system into a 1D interacting Bose gas. The latter at  $T = 0$  was exactly solved by Lieb and Liniger in 1963 by using the celebrated Bethe ansatz solution [35, 36]. The finite-

temperature thermodynamics of a 1D Bose gas was also solved a few years later by Yang and Yang, using an approach that is now commonly referred to as the Yang-Yang thermodynamic equations [37]. In the presence of a non-negligible effective range  $\xi_p \neq 0$ , a similar Bethe ansatz for all the many-body wave-functions  $\Psi$  can be constructed, by imposing a Bethe-Peierls boundary condition,  $\lim_{x \rightarrow 0^+} (1/l_p + \partial_x - \xi_p \partial_x^2) \Psi(x = |x_i - x_j|; X) = 0$  whenever two particles at  $x_i$  and  $x_j$  approach each other [18], which leads to a set of coupled equations,

$$e^{ikL} = \prod_q \frac{\xi_p (k - q)^2 - 1/|l_p| + i(k - q)}{\xi_p (k - q)^2 - 1/|l_p| - i(k - q)}. \quad (2)$$

Here, the quasi-momenta  $k$  and  $q$  take  $N$  discrete values, and  $L$  is the length of the system under a periodic boundary condition. We consider only the attractive case  $l_p < 0$ , since otherwise the energy does not have a proper thermodynamic limit [18]. At  $T = 0$ , the ground state of the system has been solved by Imambekov *et al.*, by seeking the lowest energy state of Eq. (2) [18].

At finite temperature, the Yang-Yang thermodynamic equations of a polarized Fermi gas with a finite  $\xi_p$  can also be similarly derived [19]. In the thermodynamic limit ( $N \rightarrow \infty$  and  $L \rightarrow \infty$ ), they take the exactly same form as that of bosons [18, 19], except a new kernel function,

$$\mathcal{K}(k, q) = \frac{2|l_p| [1 + |l_p|\xi_p (k - q)^2]}{[1 - |l_p|\xi_p (k - q)^2]^2 + l_p^2 (k - q)^2}. \quad (3)$$

To be more explicit, the Yang-Yang thermodynamic equations are given by ( $k_B = 1$ ) [37],

$$\begin{aligned} \epsilon(k) &= \frac{\hbar^2 k^2}{2m} - \mu - \frac{T}{2\pi} \int_{-\infty}^{\infty} \mathcal{K}(k, q) \ln \left[ 1 + e^{-\frac{\epsilon(q)}{T}} \right] dq \\ 2\pi\rho(k) \left[ 1 + e^{\frac{\epsilon(k)}{T}} \right] &= 1 + \int_{-\infty}^{\infty} \mathcal{K}(k, q) \rho(q) dq, \end{aligned} \quad (4)$$

where  $\epsilon(k)$  may be interpreted as the quasi-particle excitation energy relative to the chemical potential  $\mu$ , and  $\rho(k)$  is the quasi-momentum distribution function normalized according to  $n = N/L = \int \rho(k) dk$ . Once the Yang-Yang equations are solved, all the thermodynamic variables, for example, the total energy and pressure of the system can be calculated straightforwardly, by using  $E = [\hbar^2 L/(2m)] \int k^2 \rho(k) dk$  and  $P = [T/(2\pi)] \int \ln[1 + \exp(-\epsilon(k)/T)] dk$ , respectively [37].

To take into account the slowly-varying harmonic trapping potential in the longitudinal  $x$ -direction  $V_T(x) = m\omega_{ho}^2 x^2/2$ , which is necessary to keep atoms from escaping [2, 3], we apply the LDA approximation [20]. This amounts to setting  $\mu[n(x)] = \mu_0 - V_T(x)$ , where  $n(x)$  is the local density that is to be inversely solved once we know the relation  $\mu(n)$  from the Yang-Yang equations and  $\mu_0$  is a global chemical potential to be de-

terminated by using  $\int n(x)dx = N$  [20]. In our numerical calculations, two dimensionless interaction parameters related to the 1D scattering length  $|l_p|$  and effective range  $\xi_p$  are needed. Therefore, we define respectively  $\gamma_1 \equiv 1/(n_F|l_p|)$  and  $\gamma_2 \equiv 1/(n_F\xi_p)$ , using the peak density of a zero-temperature ideal Fermi gas at the same trap,  $n_F = \sqrt{2N}/(\pi a_{ho})$ , where  $a_{ho} = \sqrt{\hbar/(m\omega_{ho})}$  is the characteristic length along the  $x$ -axis. To be specific, we consider a polarized Fermi gas of  $N = 100$   $^6\text{Li}$  atoms under the quasi-1D confinement with  $\omega_{\perp} = 2\pi \times 200$  kHz and  $\omega_{ho} = 2\pi \times 200$  Hz, leading to a 1D effective range  $\xi_p = 1.58a_{ho}$  and  $\gamma_2 \simeq 0.14$ .

*Two-fluid hydrodynamics.* — We are particularly interested in the low-lying collective oscillations of the Fermi cloud, which are well described by a two-fluid hydrodynamic theory. At finite temperature, it takes the following form [14, 21, 22],

$$m(\omega^2 - \omega_{ho}^2)nu(x) + \frac{\partial}{\partial x} \left[ n \left( \frac{\partial P}{\partial n} \right)_{\bar{s}} \frac{\partial u(x)}{\partial x} \right] = 0, \quad (5)$$

where  $u(x)$  is a displacement field characterizing the oscillation at frequency  $\omega$ , and the derivative of the local pressure  $P$  with respect to the density  $n$  should be taken at the constant local entropy per particle  $\bar{s} = s/n$ . In free space, the displacement field  $u(x)$  takes a plane-wave solution with the dispersion  $\omega = cq$ , with a sound velocity  $c = \sqrt{(\partial P/\partial n)_{\bar{s}}/m}$ . In the presence of the confining harmonic traps, the low-lying collective modes can be solved by using a polynomial ansatz and to a good approximation, the breathing mode frequency  $\omega_b$  is given by [14],

$$\omega_b^2 = \omega_{ho}^2 + \frac{\int_{-\infty}^{\infty} [(\partial P/\partial n)_{\bar{s}}/m] n(x) dx}{\int_{-\infty}^{\infty} x^2 n(x) dx}, \quad (6)$$

which can be regarded as a finite-temperature generalization of the well-known sum-rule approach [38, 39].

*Sound speed in free space.* — In Fig. 2, we present the density dependence of the local sound velocity at some selected interaction parameters and at a typical experimental temperature (upper panel,  $T = 0.1T_F$ ) as well as at a high temperature (lower panel,  $T = T_F$ ). We note that, while the 1D effective range is directly measured in units of the harmonic oscillator length  $a_{ho}$ , the 1D scattering length is indirectly characterized using the 3D scattering volume  $-w_1/a_{\perp}^3$  for the convenience to make contact with experiments, where the magnetic field dependence of  $w_1(B)$  is known [25–28].

In the case of a negligible effective range (i.e., Figs. 2(a) and 2(d)), the sound velocity in units of the Fermi velocity,  $c/v_l(n)$ , decreases monotonically with increasing local density  $n$ . The sharp decrease at low density can be understood from the fermion-boson duality [34]. At sufficient small density  $n \ll n_F$ , the Fermi cloud lies in the fTG regime of 1D strongly interacting fermions and is equivalent to a weakly interacting Bose gas [34], in which

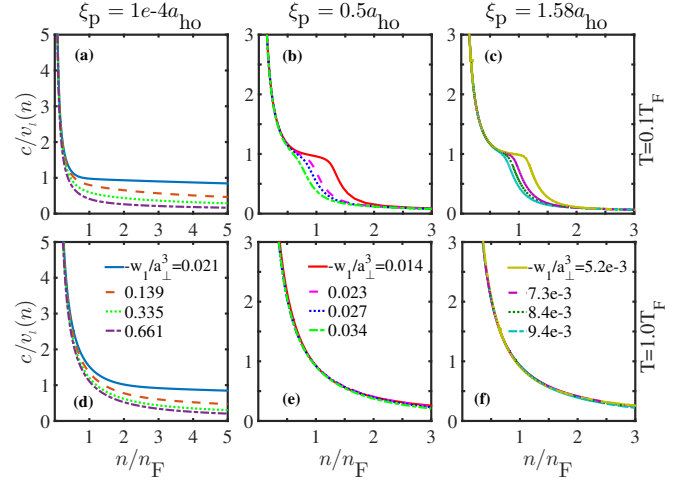


FIG. 2. (color online). Local sound velocity  $c/v_l(n)$  as a function of the local density  $n/n_F$  for three sets of effective ranges  $\xi_p = 10^{-4}a_{ho}$  [(a), (d)],  $0.5a_{ho}$  [(b), (e)], and  $1.58a_{ho}$  [(c), (f)] at low temperature  $T = 0.1T_F$  (upper panel) and high temperature  $T = T_F$  (lower panel). In each subplot, the four curves at different interaction parameters  $-w_1/a_{\perp}^3$  correspond to the four highlighted points in the curves of the squared breathing mode frequency, as shown in the insets of Fig. 3. Here,  $v_l(n) = \pi\hbar n/m$  is the local Fermi velocity and  $T_F = N\hbar\omega_{ho}$  is the Fermi temperature.

the sound velocity  $c \sim n^{1/2}$  [38, 39]. As a result, we find that  $c/v_l(n) \sim (|l_p|n)^{-1/2}$ , which quantitatively accounts for the observed rapid decrease. Instead, at large density ( $n \gg n_F$ ), the sound velocity saturates to a value that strongly depends on the scattering volume.

The density dependence of the sound velocity changes qualitatively, when the effective range comes into play (see Figs. 2(b) and 2(c)). At low temperature, in addition to the rapid decrease at low density, a plateau develops at the moderate density  $n \sim n_F$ , whose structure sensitively relies on the scattering volume  $w_1$ . By further increasing density, there is another rapid decrease. The sound velocity finally approach an asymptotically value that seems less sensitive to the scattering volume. The observed plateau in  $c/v_l(n)$  at non-negligible effective ranges might be interpreted as the emergence of the exotic super-fTG phase. Although the plateau is washed out at sufficiently large temperature, as shown in Fig. 2(e) and 2(f), it could be measured experimentally by creating a density dip at the trap center and then observing its propagation, following the routine established for a unitary Fermi gas [40].

*Density profile at  $T \neq 0$ .* — Fig. 3 reports the finite-temperature density distributions at different effective ranges, and at certain values of the interaction parameter  $-w_1/a_{\perp}^3$  as illustrated by differently colored curves. The results at a negligible effective range in Fig. 3(a) may again be understood from the fermion-boson duality [34]. At a weak interaction parameter (i.e., the blue line), the

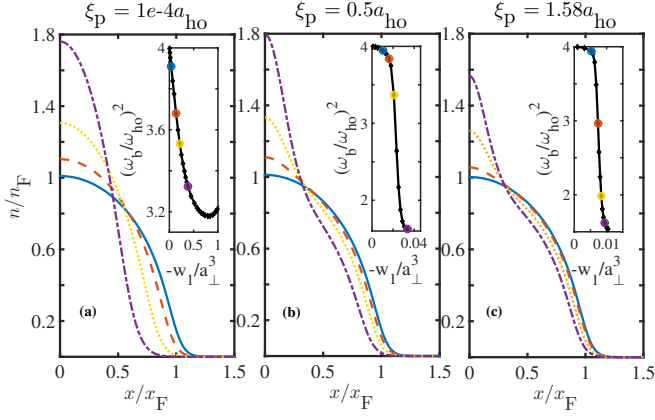


FIG. 3. (color online). Density profiles at different effective ranges: (a)  $\xi_p = 10^{-4}a_{ho}$ , (b)  $0.5a_{ho}$ , and (c)  $1.58a_{ho}$ , at  $T = 0.1T_F$ . The inset shows the squared breathing mode frequency as a function of the interaction parameter  $-w_1/a_\perp^3$ . In each subplot, the interaction parameters of colored curves can be read from the highlighted points with the same color. They are also explicitly indicated in Fig 2. Here,  $x_F = \sqrt{2N}a_{ho}$  is the radius of an ideal trapped Fermi gas at zero temperature.

profile is simply an ideal Fermi gas distribution. When the interaction becomes more attractive, as described by the Cheon-Shigehara (CS) model [34], the Fermi cloud is dual to an interacting Bose gas with an appropriate repulsion strength  $\propto |l_p|^{-1} \propto |w_1|^{-1}$ . Thus, the profile becomes narrower and the peak density is higher, behaving exactly the same as a 1D Bose gas [20].

In the presence of sizable effective ranges, as shown in Figs. 3(b) and 3(c) for  $\xi_p = 0.5a_{ho}$  ( $\gamma_2 \simeq 0.44$ ) and  $\xi_p = 1.58a_{ho}$  ( $\gamma_2 \simeq 0.14$ ), the shape of the density profile is greatly altered, even by a small increase in the interaction parameter  $-w_1/a_\perp^3$ . The peak density increases significantly, probably due to the enhanced attraction by the finite effective-range. Furthermore, the profile at large effective range clearly shows a bimodal distribution. The dramatic change in the density distribution comes along with a sharp decrease in the breathing mode frequency, as reported in the two insets, which we shall now discuss in greater detail. We note that, at zero temperature, similar changes have been observed by Imambekov and co-workers [18].

*Breathing mode at  $T \neq 0$ .* — With the sound velocity  $c(x)$  and density distribution  $n(x)$  at hand, we calculate straightforwardly the finite-temperature breathing mode frequency using the generalized sum-rule approximation Eq. (6). The measurement of collective excitations proved to be a powerful and convenient way to characterize possible new quantum states of matter arising from the intriguing effects of interatomic interactions [38, 41]. In an interacting 1D Bose gas, the transition from the weakly-interacting regime to the TG regime for impenetrable bosons is characterized by a nontrivial but smooth evolution of the squared breathing mode

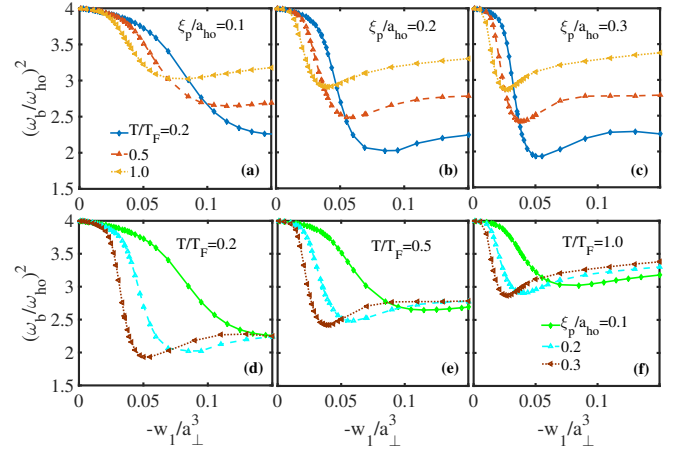


FIG. 4. (color online). The squared breathing mode frequencies  $(\omega_b/\omega_{ho})^2$  as a function of the interaction parameter  $-w_1/a_\perp^3$ , at different effective ranges (upper panel (a)-(c)) or at different temperatures (lower panel, (d)-(e)), as indicated.

frequency, which starts at about 4 in the ideal gas limit, decreases to 3 at the mean-field Gross-Pitaevskii regime, and then increases back to 4 in the TG limit [8, 15]. At a sufficiently small effective range, we have checked the above smooth evolution of the mode frequency, as anticipated from the fermion-boson mapping [34].

Fig. 4 presents the breathing mode frequency at some finite effective ranges and finite temperatures. Typically, we find that the mode frequency experiences a sudden drop at a certain critical value of  $-w_1/a_\perp^3$ , after which the frequency slowly increases. This sudden change could be viewed as a clear signature of the appearance of the super-fTG phase. It is readily seen that this sudden-drop feature is enhanced by a large effective range, which also leads to a minimum squared frequency as small as  $2\omega_{ho}^2$ . A finite temperature tends to significantly lift the minimum frequency. However, the sudden-drop structure is merely unchanged.

A typical phase diagram of the 1D polarized Fermi cloud can then be summarized, as shown earlier in Fig. 1 for an experimentally reachable temperature  $T = 0.1T_F$ . At large enough  $\gamma_2$  (i.e. negligible effective range), the squared frequency  $(\omega_b/\omega_{ho})^2$  of the system shows a reentrant behavior, valuing about 4 in the weakly-interacting limit, changing to 3 at the intermediate regime and finally returning back to 4 in the fTG limit, as a result of the duality to a 1D Bose gas. In contrast, at sufficiently small  $\gamma_2$  (i.e. sizable effective range), with increasing  $|l_p|$  or decreasing  $\gamma_1$ , the frequency ratio loses the reentrant behavior and drops sharply to a much lower value at a critical interaction parameter, thereby signifying the phase transition to the super-fTG phase. At low temperature, the critical interaction parameter may be estimated from

the ground-state energy [18],

$$\left[ \frac{\gamma_1 \gamma_2}{4\pi^2} \right]_{\text{super-fTG}} \simeq 1 + \frac{\zeta(-1/2) a_{\text{ho}}}{4\pi \sqrt{N} a_{\perp}} \gamma_2, \quad (7)$$

This estimation - illustrated by a black dashed line in the figure - agrees qualitatively well with our results and encloses the blue super-fTG area with small breathing mode frequencies. For a  $^6\text{Li}$  polarized Fermi gas near the  $p$ -wave Feshbach resonance at  $B_0 = 215.0$  G, where  $\gamma_2 \simeq 0.14$ , we find that  $(\gamma_1)_{\text{super-fTG}} \simeq 275$  or  $(a_{\perp}^3/w_1)_{\text{super-fTG}} \simeq -118$ . This corresponds to a detuning from the resonance at about 0.05 G.

*Summary.* — We have investigated the thermodynamics and dynamics of spin-polarized fermions with a resonant  $p$ -wave interaction under a one-dimensional harmonic confinement at finite temperature, by solving the exact Yang-Yang thermodynamic equations and two-fluid hydrodynamic equation. We have shown that there are distinct features in the density distribution and collective mode frequency for identifying an exotic effective-range-induced super fermionic Tonks-Girardeau state. These features are not sensitive to the presence of a finite temperature. As a result, our predictions are readily testable with ultracold  $^6\text{Li}$  or  $^{40}\text{K}$  atoms near a  $p$ -wave Feshbach resonance at an experimental achievable temperature  $T \simeq 0.1T_F$ .

We thank very much Professor Xi-Wen Guan for his explanation on the Yang-Yang thermodynamics of the 1D  $p$ -wave Fermi gas with the effective range of the interaction included. This work was supported by the ARC Discovery Projects: DP140100637 and FT140100003 (XJL), FT130100815 and DP140103231 (HH).

---

\* hhu@swin.edu.au

- [1] B. Sutherland, *Beautiful Models: 70 Years of Exactly Solved Quantum Many-Body Problems* (World Scientific, 2004).
- [2] S. Richard, F. Gerbier, J. H. Thywissen, M. Hugbart, P. Bouyer, and A. Aspect, Phys. Rev. Lett. **91**, 010405 (2003).
- [3] H. Moritz, T. Stoferle, M. Köhl, and T. Esslinger, Phys. Rev. Lett. **91**, 250402 (2003).
- [4] B. Paredes, A. Widera, V. Murg, O. Mandel, S. Fölling, I. Cirac, G. V. Shlyapnikov, T. W. Hansch, and I. Bloch, Nature (London) **429**, 277 (2004).
- [5] T. Kinoshita, T. Wenger, and D. S. Weiss, Science **305**, 1125 (2004).
- [6] H. Moritz, T. Stoferle, K. Günter, M. Köhl, and T. Esslinger, Phys. Rev. Lett. **94**, 210401 (2005).
- [7] K. Günter, T. Stoferle, H. Moritz, M. Köhl, and T. Esslinger, Phys. Rev. Lett. **95**, 230401 (2005).
- [8] E. Haller, M. Gustavsson, M. J. Mark, J. G. Danzl, R. Hart, G. Pupillo, and H.-C. Nägerl, Science **325**, 1224 (2009).
- [9] B. Fang, G. Carleo, A. Johnson, and I. Bouchoule, Phys. Rev. Lett. **113**, 035301 (2014).
- [10] For a review, see, for example, M. A. Cazalilla, R. Citro, T. Giamarchi, E. Orignac, and M. Rigol, Rev. Mod. Phys. **83**, 1405 (2011); X.-W. Guan, M. T. Batchelor, and C. Lee, Rev. Mod. Phys. **85**, 1633 (2013).
- [11] M. Girardeau, J. Math. Phys. **1**, 516 (1960).
- [12] K. Kheruntsyan, D. Gangardt, P. Drummond, and G. Shlyapnikov, Phys. Rev. Lett. **91**, 040403 (2003).
- [13] A. Minguzzi and D. M. Gangardt, Phys. Rev. Lett. **94**, 240404 (2005).
- [14] H. Hu, G. Xianlong, and X.-J. Liu, Phys. Rev. A **90**, 013622 (2014).
- [15] X.-L. Chen, Y. Li, and H. Hu, Phys. Rev. A **91**, 063631 (2015).
- [16] G. E. Astrakharchik, J. Boronat, J. Casulleras, and S. Giorgini, Phys. Rev. Lett. **95**, 190407 (2005).
- [17] M. T. Batchelor, M. Bortz, X.-W. Guan, and N. Oelkers, J. Stat. Mech. **2005**, L10001 (2005).
- [18] A. Imambekov, A. A. Lukyanov, L. I. Glazman, and V. Gritsev, Phys. Rev. Lett. **104**, 040402 (2010).
- [19] X.-W. Guan, private communication.
- [20] V. Dunjko, V. Lorent, and M. Olshanii, Phys. Rev. Lett. **86**, 5413 (2001).
- [21] E. Taylor, H. Hu, X.-J. Liu, and A. Grin, Phys. Rev. A **77**, 033608 (2008).
- [22] E. Taylor, H. Hu, X.-J. Liu, L. P. Pitaevskii, A. Grin, and S. Stringari, Phys. Rev. A **80**, 053601 (2009).
- [23] L. D. Landau and E. M. Lifshitz, *Quantum Mechanics: Non-relativistic Theory*, Vol. 3 (Elsevier, 2013) p.522.
- [24] C. Chin, R. Grimm, P. Julienne, and E. Tiesinga, Rev. Mod. Phys. **82**, 1225 (2010).
- [25] J. Zhang, E. G. M. van Kempen, T. Bourdel, L. Khaykovich, J. Cubizolles, F. Chevy, M. Teichmann, L. Tarruell, S. J. J. M. F. Kokkelmans, and C. Salomon, Phys. Rev. A **70**, 030702(R) (2004).
- [26] C. Ticknor, C. A. Regal, D. S. Jin, and J. L. Bohn, Phys. Rev. A **69**, 042712 (2004).
- [27] C. H. Schunck, M. W. Zwierlein, C. A. Stan, S. M. F. Raupach, and W. Ketterle, Phys. Rev. A **71**, 045601 (2005).
- [28] J. Fuchs, C. Ticknor, P. Dyke, G. Veeravalli, E. Kuhnle, W. Rowlands, P. Hannaford, and C. J. Vale, Phys. Rev. A **77**, 053616 (2008).
- [29] B. E. Granger and D. Blume, Phys. Rev. Lett. **92**, 133202 (2004).
- [30] L. Pricoupenko, Phys. Rev. Lett. **100**, 170404 (2008).
- [31] M. Olshanii, Phys. Rev. Lett. **81**, 938 (1998).
- [32] S.-G. Peng, S. Tan, and K. Jiang, Phys. Rev. Lett. **112**, 250401 (2014).
- [33] T. Cheon and T. Shigehara, Phys. Lett. A **243**, 111 (1998).
- [34] T. Cheon and T. Shigehara, Phys. Rev. Lett. **82**, 2536 (1999).
- [35] E. H. Lieb and W. Liniger, Phys. Rev. **130**, 1605 (1963).
- [36] E. H. Lieb, Phys. Rev. **130**, 1616 (1963).
- [37] C. N. Yang and C. P. Yang, J. Math. Phys. **10**, 1115 (1969).
- [38] F. Dalfovo, S. Giorgini, L. P. Pitaevskii, and S. Stringari, Rev. Mod. Phys. **71**, 463 (1999).
- [39] L. P. Pitaevskii and S. Stringari, *Bose-Einstein Condensation*, 116 (Oxford University Press, 2003) Chap. 4.
- [40] J. Joseph, B. Clancy, L. Luo, J. Kinast, A. Turlapov, and J. E. Thomas, Phys. Rev. Lett. **98**, 170401 (2007).
- [41] H. Hu, A. Minguzzi, X.-J. Liu, and M. P. Tosi, Phys.

Rev. Lett. **93**, 190403 (2004).